4-2017

Hydraulics Near Unscreened Diversion Pipes in Open Channels: Large Flume Experiments

Ali Ercan
University of California, Davis

M. Levent Kavvas
University of California, Davis

Kara Carr
University of California, Davis

Zachary Hockett
University of California, Davis

Houssein Bandeh
University of California, Davis

See next page for additional authors

Authors
Ali Ercan, M. Levent Kavvas, Kara Carr, Zachary Hockett, Houssein Bandeh, Timothy D. Mussen, Dennis E. Cocherell, Jamilynn B. Poletto, Joseph J. Cech Jr., and Nann A. Fangue

Published in *Journal of the American Water Resources Association* (JAWRA) 53:2 (April 2017), pp 431–441.
doi 10.1111/1752-1688.12503

Submitted March 22, 2016; accepted November 30, 2016; published 6 February 2017.

Hydraulics Near Unscreened Diversion Pipes in Open Channels: Large Flume Experiments

Ali Ercan,[1] M. Levent Kavvas,[1] Kara Carr,[1] Zachary Hockett,[1] Hossein Bandeh,[1] Timothy D. Mussen,[2] Dennis Cocherell,[3] Jamilynn B. Poletto,[3,4] Joseph J. Cech, Jr.,[3] and Nann A. Fangue[3]

1 Department of Civil and Environmental Engineering, University of California, Davis, California 95616

2 Sacramento Regional County Sanitation District, Sacramento, California 95827

3 Department of Wildlife, Fish, and Conservation Biology, University of California, Davis, California 95616

4 School of Natural Resources, University of Nebraska-Lincoln, 3300 Holdrege Street, Lincoln, Nebraska 68583

Corresponding author — A. Ercan, *email* aercan@ucdavis.edu

Abstract

Most of the water diversions on the Sacramento and San Joaquin Rivers (California, United States) and their tributaries are currently unscreened. These unscreened diversions are commonly used for irrigation and are potentially harmful to migrating and resident fishes. A large flume (test section: 18.29 m long, 3.05 m wide and 3.20 m high) was used to investigate the hydraulic fields near an unscreened water diversion under ecologically and hydraulically relevant diversion rates and channel flow characteristics. We investigated all combinations of three diversion rates (0.28, 0.42, and 0.57 m^3/s) and three sweeping velocities (0.15, 0.38, and 0.61 m/s), with one additional test at 0.71 m^3/s and 0.15 m/s. We measured the three-dimensional velocity field at seven cross sections near a diversion pipe and constructed regression equations of the observed maximum velocities near the pipe. Because the velocity components in three directions (longitudinal, transverse, and vertical) were significantly greater near the diversion pipe inlet compared with those farther from it, they cannot be neglected in the modeling and design of fish guidance and protection devices for diversion pipes. Our results should be of great value in quantifying the hydraulic fields that are formed around fish guidance devices to design more effective protection for fishes from entrainment into unscreened water-diversion pipes.

Keywords: fish, rivers/streams, hydraulic structures, hydrodynamics, open channel flow, fish entrainment, fish passage, flume experiments

Introduction

According to the Central Valley Project Improvement Act (CVPIA, 1992), the United States (U.S.) Secretary of the Interior is authorized and directed to assist the State of California in efforts to develop and implement measures to avoid losses of juvenile anadromous fishes resulting from unscreened or inadequately screened diversions on the Sacramento and San Joaquin Rivers, their tributaries, the Sacramento- San Joaquin Delta, and Suisun Marsh. Such measures include construction of screens on unscreened diversions, rehabilitation of existing screens, replacement of existing nonfunctioning screens, and relocation of diversions to less fishery-sensitive areas. Most of the smaller sized irrigation pipes used in these waterways are currently unscreened (CalFish, 2012). These unscreened water diversion pipes are potentially harmful to migrating and resident fishes, including several threatened or endangered species (Turnpenny *et al.*, 1998; Nobriga *et al.*, 2004; King and O'Connor, 2007; Gale *et al.*, 2008; Kimmerer, 2008; Grimaldo *et al.*, 2009; Mussen *et al.*, 2014a; and Poletto *et al.*, 2014, 2015). Fish entrained into these diversions (drawn in with water inflow) are either killed directly by physical damage from the pumps, or indirectly through stranding in the seasonally irrigated canals, ditches, and fields supplied by the water diversions (Mussen *et al.*, 2013). Because these water diversions are often unpermitted and unrecorded (Bowen, 2004), their cumulative effect on fish populations is difficult to quantify, though estimates of the number of water diversions in the Sacramento-San Joaquin watershed alone are in excess of 3,300 (Herren and Kawasaki, 2001), with the vast of majority of these unscreened.

We investigated the relationship between the hydraulic fields surrounding an unscreened diversion pipe and fish swimming behavior under relevant diversion and channel flow characteristics, using a large flume at the J. Amorocho Hydraulics Laboratory (JAHL) of University of California, Davis. Results of the fish behavior and entrainment risks near unscreened water diversions with and without various fish protection devices were reported recently by Mussen *et al.* (2013, 2014a, b, 2015) and Poletto *et al.* (2014, 2015). Mussen *et al.* (2013) evaluated juvenile Chinook salmon (mean fork lengths between 12.5 and 13.3 cm) entrainment risk and their behavioral responses to an unscreened diversion pipe under various channel flow and diversion rate conditions during day, night, and in turbid water conditions. Mussen *et al.* (2014a) estimated that after outmigrating juvenile green sturgeon (35 ± 0.6 cm mean fork length) passed within 1.5 m of three active water-diversion pipes, up to 52% of these fish could be entrained, which suggests that green sturgeon can be highly vulnerable to unscreened water-diversion pipes under particular flow conditions.

In this article, we report the hydraulic conditions near a 0.46-m-diameter diversion pipe under ecologically and hydraulically representative diversion rates and channel flow characteristics in a large experimental flume (test section: 18.29 m long, 3.05 m wide, and 3.20 m high). We conducted laboratory- based experiments to characterize and quantify the three-dimensional (3-D) flow fields associated with an unscreened, 0.46-m-diameter, water-diversion pipe with a 26.6°-sloped bank configuration to simulate a typical over-the-levee water-diversion pipe. Our results should help managers understand the relationships between the hydraulic fields and fish-swimming behavior near unscreened diversions under relevant inflow rates and channel flow characteristics, and assist in designing fish-guidance and protection devices to protect fishes from entrainment into unscreened water-diversion pipes.

Description of the Flume and Measurements

The experimental flume rests on a 18.29-m-long × 18.29-m-wide reinforced concrete structure at the JAHL at the University of California, Davis (Figure 1). The test section of the flume was 18.29 m long, 3.05 m wide, and 3.20 m high. Water was circulated through the flume using two 0.61-m-diameter pipes, one 1.22-m-diameter pipe, and three pumps that were capable of moving 3.26 m^3/s of water. Water, after entering the head tank (12.19 m length, 1.83 m width), flowed through vertical bar racks into the 3.05-m-wide flume channel. The head tank and the bar racks functioned to minimize the turbulence and evenly distribute water in the channel. Water discharge to the flume channel was controlled, using variable speed motors. Different water depths in the flume channel (1.8 to 2.4 m) were achieved via weir position adjustment at the downstream end of the flume. An unscreened diversion pipe (0.46 m diameter) was installed at the midpoint of the flume with a sloped configuration to simulate a typical, over-the-levee diversion pipe (**Figure 1**). The diversion water was returned into the (downstream) tail tank by the head difference between the water in the flume and water in the tail tank. Thus, diverted fish were not harmed because there was no pump in the diversion pipe. Diverted water was mixed

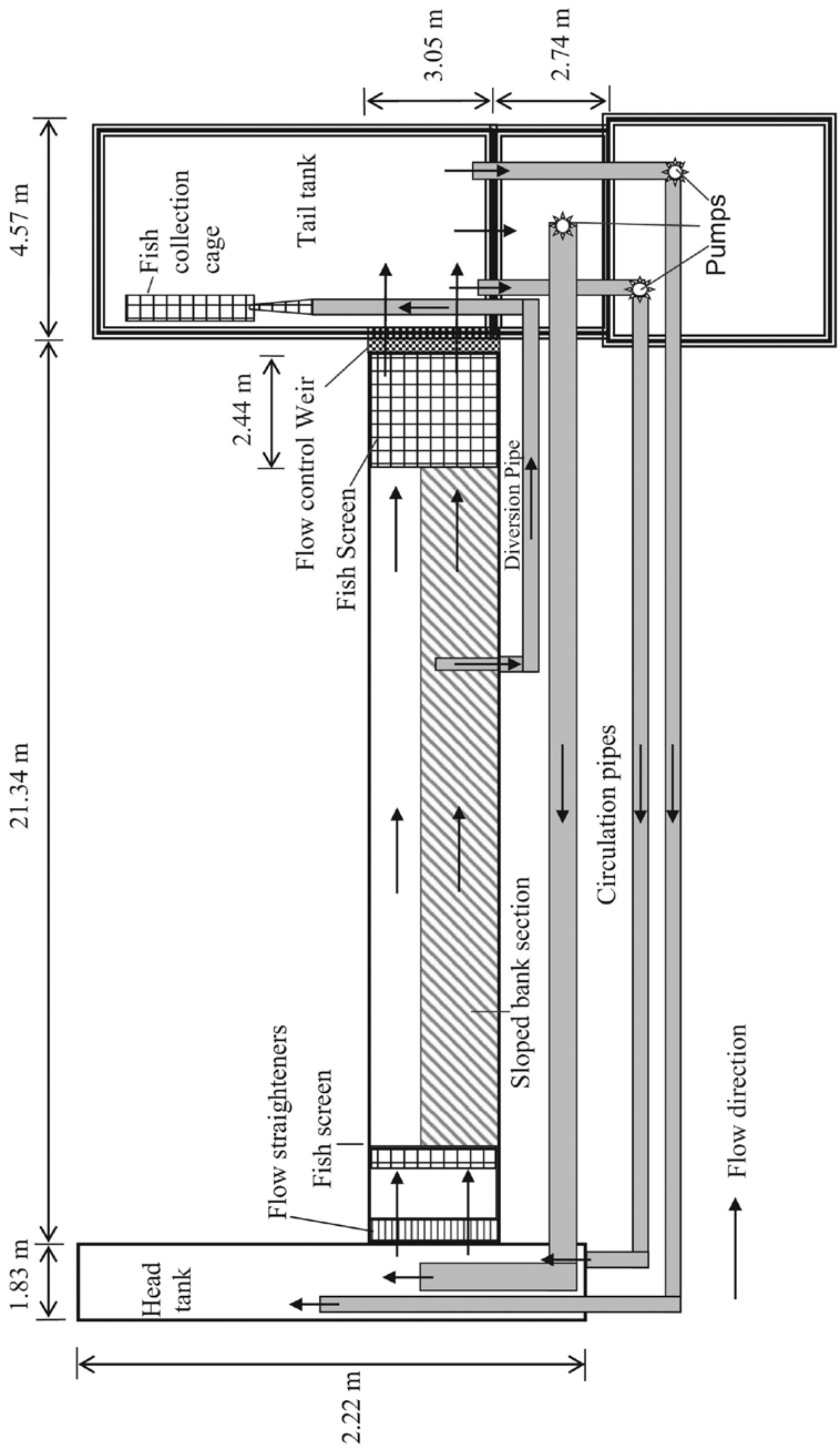

Figure 1. Plan View of Experimental Flume Setup.

with that from the flume in the tail tank and pumped back through the circulation pipes (**Figure 2**). During fish-swimming experiments, the fish were restricted to swimming in the main channel by upstream and downstream stainless steel 6.4 × 6.4 mm welded wire mesh screens. Details of the fish screens and fish release and collection mechanisms in the experimental flume were described by Mussen *et al.* (2013).

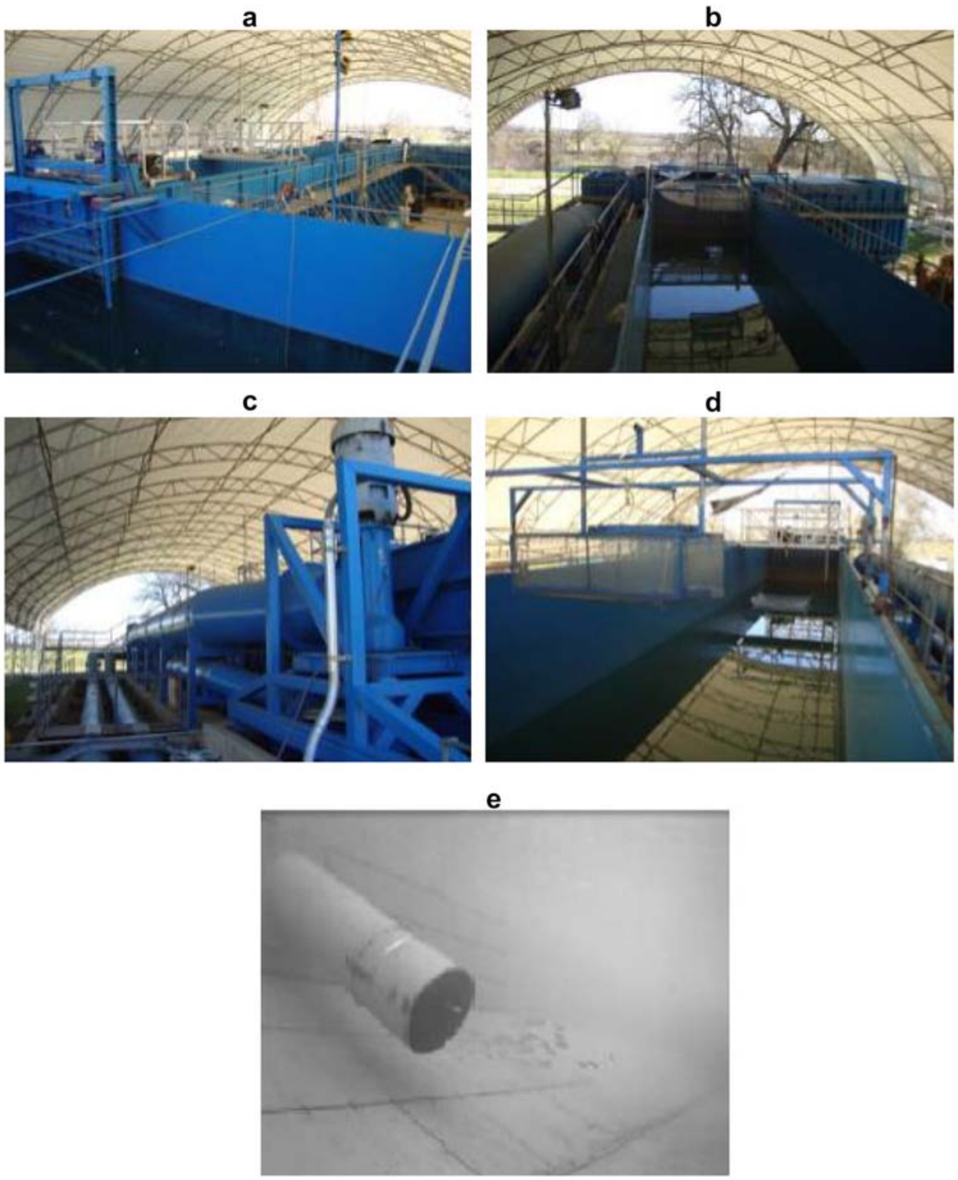

Figure 2. Photographs of the experimental flume: **(a)** Photograph taken from the tail tank looking into upstream, **(b)** Photograph taken over the weir looking into upstream flume and the head tank, **(c)** Photograph showing the circulating and diversion pipes, **(d)** Photograph taken from the head tank looking into downstream flume, **(e)** Photograph showing the underwater view of the diversion pipe.

The detailed 3-D velocity field was measured at seven cross sections in the flume. Main flow direction components (*x*, *y*, *z* directions) and the plan view of the seven measurement cross sections (S1, S2, S3, S4, S5, S6, S7) are depicted in Figure 3. The cross section S4 was located at the center of the diversion pipe, at $x = 0$. The *x*-axis was negative in the upstream and positive in the downstream direction of the diversion pipe. The cross section S1 (or $x = -1.83$ m) was located 1.83 m upstream of S4 and the cross section S7 (or $x = 1.83$ m) was 1.83 m downstream of S4. The cross sections S2 and S6 were 0.76 m upstream and downstream of the center of the diversion pipe, respectively, while the S3 and S5 cross sections were 0.38 m upstream and downstream of the diversion pipe's center, respectively. The transverse $+y$ direction was toward the flume wall with the diversion pipe, and the vertical $+z$ direction was toward the water surface. A positive or negative sign preceding the velocity measure represents the direction of the velocity.

Moreover, once fish entrainment-starting locations and their distances from the center of the diversion pipe inlet for juvenile Chinook salmon were identified through the video analysis as described in detail at Mussen *et al.* (2013), the 3-D velocities were measured at these entrainment locations. These entrainment velocities were then analyzed based on the probability of the exceedance concept.

Instrumentation and Data Processing

Water flow conditions were measured, using a 3-D SonTek® ADV probe, which is capable of measuring the 3-D velocities at 25 Hz. The accuracy of the device was ±1% of the measured velocity. Velocity contours of cross sections were generated by 2-D Kriging interpolation. To account for the velocity fluctuations through time at a fixed location in the flume, the 3-D velocity field was averaged over a 15-s duration. The accuracy of the SonTek ADV probe was ±1% of the measured velocity (SonTek Technical Documentation, September 2001).

Results and Discussion

A total of ten hydraulic experiments were conducted, as listed in **Table 1**: nine experiments investigated all combinations of diversion rates (0.28, 0.42, and 0.57 m^3/s) with three representative sweeping velocities (0.15, 0.38, and 0.61 m/s). One additional test was conducted at 0.71 m^3/s and 0.15 m/s. The channel sweeping velocity (V_{swp}) was the average, longitudinal velocity in the upstream section of the flume, where the diversion pipe had no hydraulic influence. The flow combinations utilized in this study provide a range of flows commonly present at unscreened water diversions on the middle and

Table 1. Description of the Hydraulic Tests.

Test Number	*Diversion Rate (m^3/s)*	*Sweeping Velocity (m/s)*
1	0.28	0.15
2	0.42	0.15
3	0.42	0.38
4	0.42	0.61
5	0.57	0.15
6	0.57	0.38
7	0.57	0.61
8	0.28	0.38
9	0.28	0.61
10	0.71	0.15

lower Sacramento River main stem (Dan Meier, U.S. Fish and Wildlife Service, personal communication).

The 3-D velocity field at a cross section is represented by a plot with contours of the *x*-direction velocities superimposed on the *y*- and *z*-direction velocity vectors in the cross section. The seven plots on the left sides of **Figures 4-6** are used to present the 3-D velocity fields measured in the flume for Test 5 (0.15 m/s sweeping velocity and 0.57 m^3/s diversion rate) at the seven cross sections S1, S2, S3, S4, S5, S6, and S7 (as shown in **Figure 3**). The seven plots

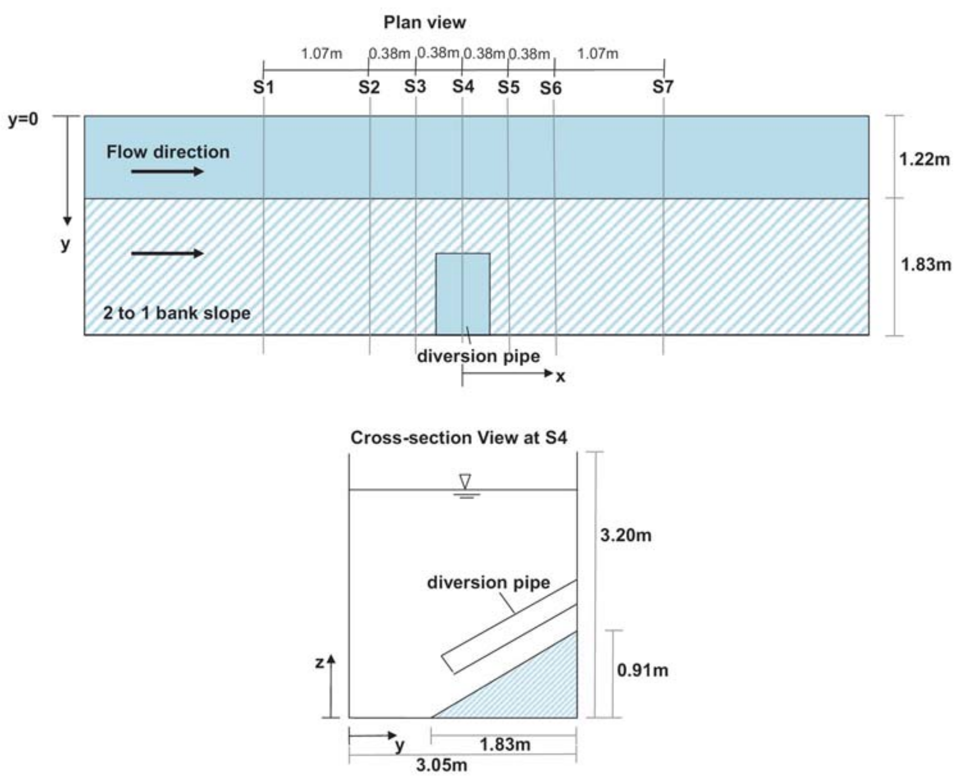

Figure 3. Main Flow Direction Components (*x*, *y*, *z* directions) and the Measurement Cross Sections.

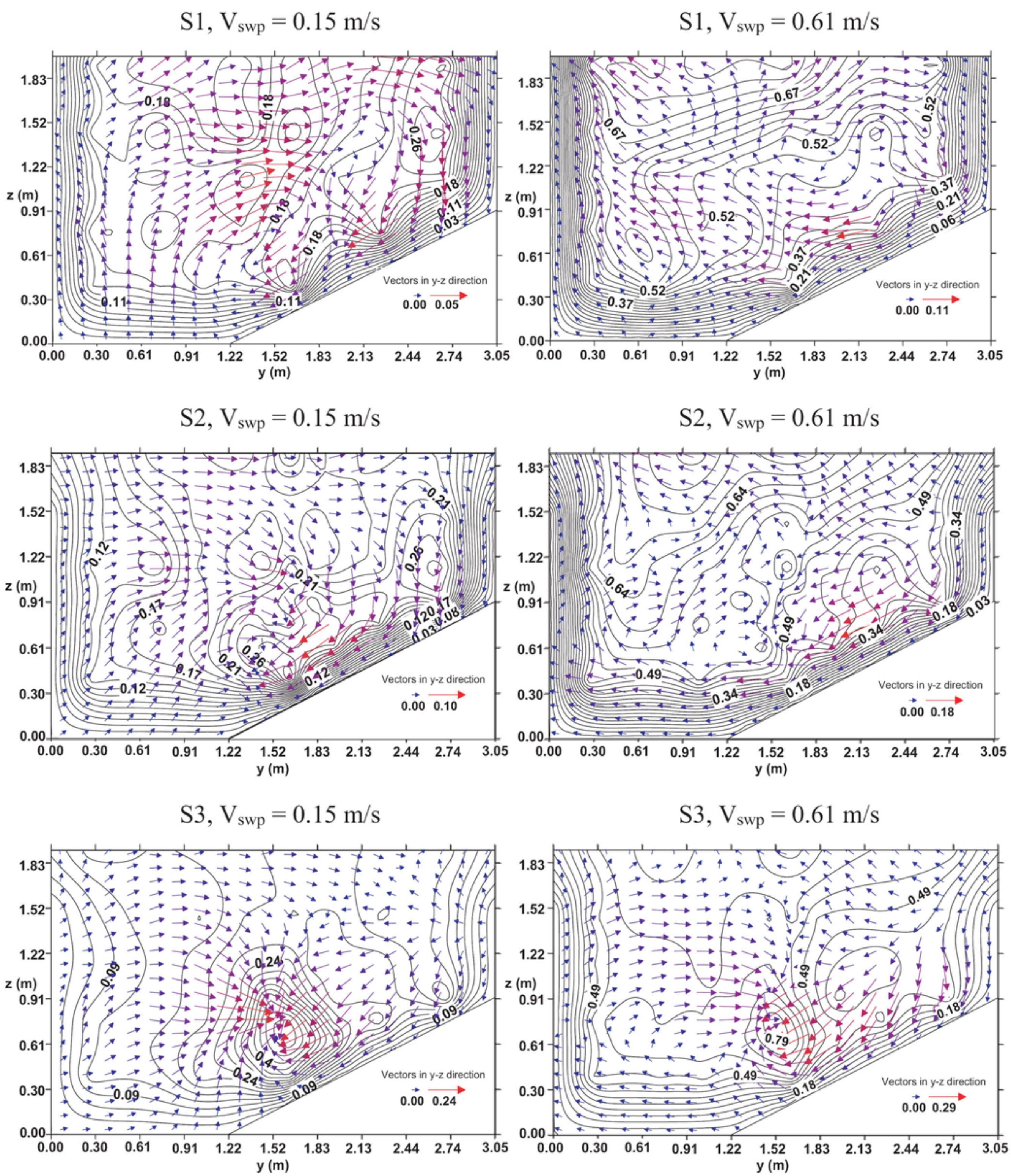

Figure 4. Contours of *x*-Direction Velocities Superimposed on Velocity Vectors of *y*- and *z*-Directions at Cross Sections S1, S2, and S3 for 0.15 and 0.61 m/s Sweeping Velocities with a 0.57 m^3/s Diversion Rate (*i.e.,* figures for Test 5 on the left and Test 7 on the right).

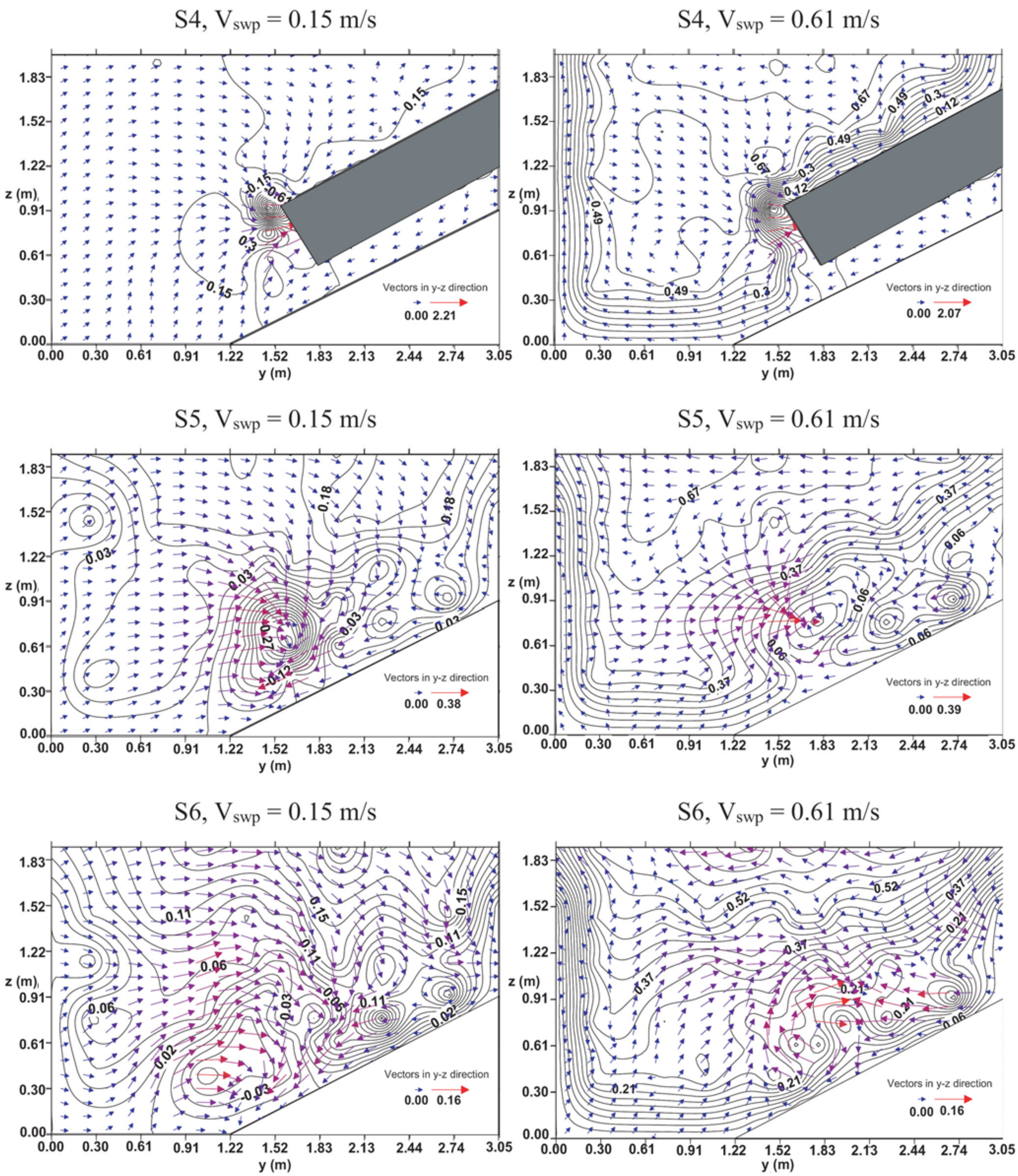

Figure 5. Contours of *x*-Direction Velocities Superimposed on Velocity Vectors of *y*- and *z*-Directions at Cross Sections S4, S5, and S6 for 0.15 and 0.61 m/s Sweeping Velocities with a 0.57 m^3/s Diversion Rate (*i.e.,* figures for Test 5 on the left and Test 7 on the right).

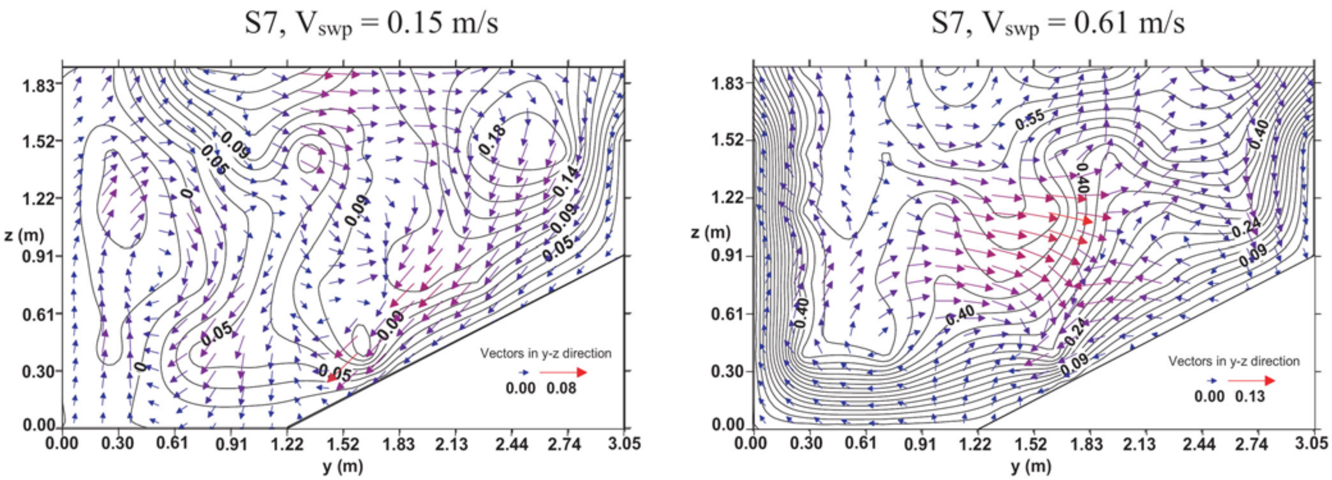

Figure 6. Contours of *x*-Direction Velocities Superimposed on Velocity Vectors of *y*- and *z*-Directions at Cross Section S7 for 0.15 and 0.61 m/s Sweeping Velocities with a 0.57 m^3/s Diversion Rate (*i.e.,* figures for Test 5 on the left and Test 7 on the right).

on the right sides of **Figures 4-6** are used to present the 3-D velocity fields measured in the flume for Test 7 (0.61 m/s sweeping velocity and 0.57 m^3/s diversion rate). These figures show how the hydraulic fields varied with respect to changes in sweeping velocity. Firstly, longitudinal velocities (V_x) along the main flow direction increased at the cross section where the diversion pipe was located because the cross sectional area narrowed down due to the diversion pipe.

Secondly, secondary velocities (*i.e.*, transverse direction velocity V_y, and vertical direction velocity V_z) increased from upstream to the location of the diversion pipe (from cross section S1 to S4) due to the diversion flow which was perpendicular to the sweeping velocity direction. Secondary velocities decreased from the location of the diversion pipe to downstream (from cross section S4 to S7). Thus, all of the velocity components, *i.e.*, in the longitudinal, transverse, and vertical directions, were significantly increased in the vicinity of the diversion pipe inlet. Consequently, velocity components in longitudinal (*x*-), transverse (*y*-), and vertical (*z*-) directions need to be considered in the modeling and design of fish guidance and protection devices for the diversion pipes. Secondary velocities (*y*- and *z*-direction velocities) developed in the vicinity of the diversion pipe are mainly due to the suction of the water by the diversion pipe and the obstruction effect of it. Transverse (*y*-) and vertical (*z*-) direction velocities were negligible at 1.83 m upstream and downstream of the diversion pipe when compared to those at the proximity of the diversion pipe.

Thirdly, the starting locations of the fish entrainment events that were reported by Mussen *et al.* (2013) were directly correlated with the hydraulic zone of influence of the diversion pipe, which varied with the sweeping velocity for a fixed diversion rate, as depicted in the velocity contours and vectors of cross sections S3, S4, and S5 in **Figures 4 and 5**. Because different sweeping velocities have different inertias in the longitudinal direction, a fixed diversion rate resulted in varying hydraulic zones of influence under changing sweeping velocities. Additionally, at a fixed sweeping velocity, the higher diversion rate resulted in an increased hydraulic zone of influence. This intuitive result was also supported by changes in the average distances where fish started to become entrained into the diversion pipe, as reported by Mussen *et al.* (2013). As reported in Mussen *et al.* (2013, Figure 8), fish entrainment starting distances from the center of the diversion pipe inlet increased from 30 cm at 0.42 m^3/s to 36 cm at 0.57 m^3/s at a sweeping velocity of 0.15 m/s, and from 36 cm at 0.42 m^3/s to 37 cm at 0.57 m^3/s at a sweeping velocity of 0.61 m/s.

Moreover, for the 0.57 m^3/s diversion rate shown in **Figures 4-6**, the diversion pipe created different velocity gradients under the 0.15 and 0.61 m/s sweeping velocities. More specifically, under the constant 0.57 m^3/s diversion rate there is an average suction velocity of 3.43 m/s. Therefore, the 0.15 m/s sweeping velocity resulted in a higher velocity gradient within the channel toward the diversion pipe compared to the 0.61 m/s sweeping velocity. Juvenile Chinook salmon (Mussen *et al.*, 2013) and juvenile green sturgeon (Mussen *et al.*, 2014a) were more likely to become entrained by the sudden increase in the velocity gradient generated by the diversion at the 0.15 m/s sweeping velocity compared to the more gradual increase in velocity generated at 0.61 m/s.

Lastly, the highest velocity magnitudes [$V_{mag} = (V_x^2 + V_y^2 + V_z^2)^{1/2}$] were observed in the vicinity of the diversion pipe because stream-wise velocities (V_x) and secondary velocities (*i.e.*, transverse direction velocity V_y and vertical velocity V_z) were highest in the vicinity of the diversion pipe, as discussed above. Additionally, magnitudes of the velocities downstream of the diversion pipe were less than those upstream because of the diverted water, the hydraulic energy losses due to the flume walls at the bed and sides, and the obstruction effect of the diversion pipe.

The maximum values of positive and negative (reverse direction) transverse (*y*-) and vertical (*z*-) direction velocities in the vicinity of the diversion pipe (at x = –0.38, 0, 0.38 m) were nondimensionalized with respect to sweeping velocity V_{swp} and reported in **Figures 7 and 8**, respectively. The corresponding values of the velocity magnitudes are presented in **Figure 9**. Quadratic or cubic regression relations between the nondimensional velocities in m/s and the diversion rates in m^3/s are also reported in **Figure 7**

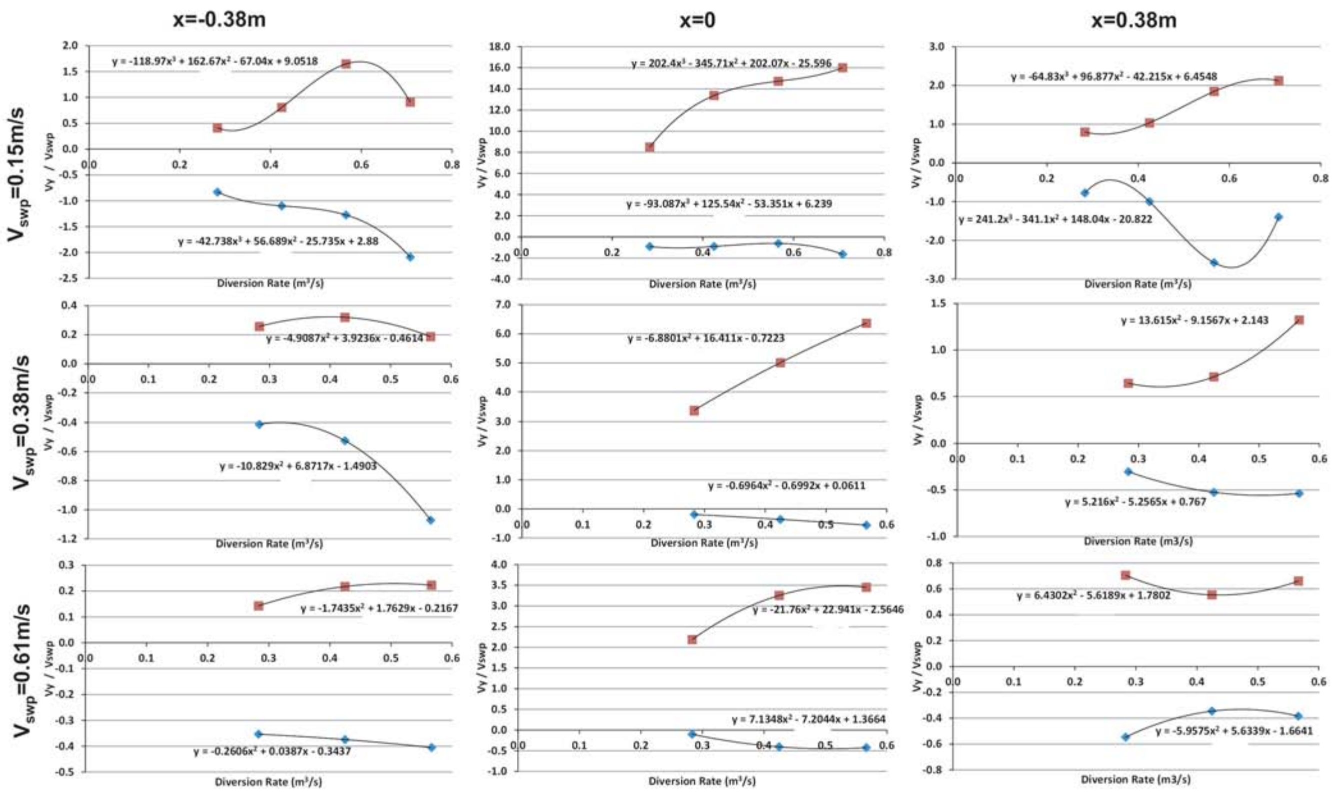

Figure 7. Maximum Values of Positive and Negative Nondimensional Transverse (*y*-) Direction Velocities V_y/V_{swp} for Various Diversion Rates and Sweeping Velocities at x = –0.38, 0, 0.38 m (scales of *y*-axis are different for each figure).

for *y*-direction velocities, in **Figure 8** for *z*-direction velocities, and in **Figure 9** for velocity magnitudes. The regression equations demonstrate the trend within the measured velocities and provide the exact measured velocities for the tested diversion rates (0.28, 0.42, and 0.57 m^3/s) but may not be accurate for other diversion rates. The 3-D velocity field (**Figures 4-6**), the maximum values of positive and negative velocities (**Figures 7-9**), and the regression relations provide detailed description of the hydraulic field around the diversion pipe.

Probability of exceedance of juvenile Chinook salmon entrainment velocities in *x*-, *y*-, *z*-directions, and the corresponding velocity magnitudes are depicted in Figure 10. These velocities correspond to the fish entrainment starting locations reported in Mussen *et al.* (2013). The mean entrainment velocity was estimated as 0.50 m/s in the longitudinal (*x*-) direction, 0.39 m/s in the transverse (*y*-) direction, 0.20 m/s in the vertical (*z*-) direction, and 0.74 m/s for the resultant velocity magnitude. Furthermore, the median of the entrainment velocity was estimated as 0.40 m/s in the longitudinal (*x*-)

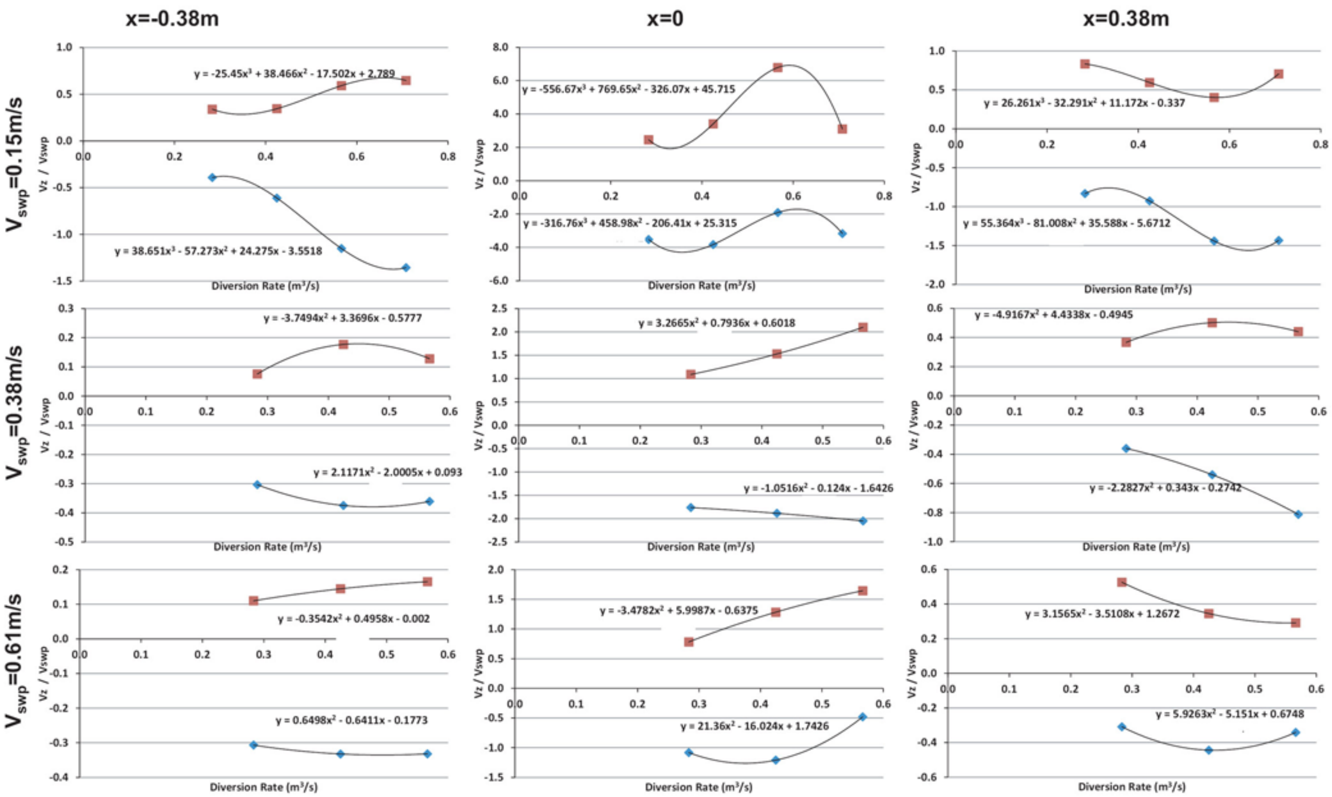

Figure 8. Maximum Values of Positive and Negative Nondimensional *z*-Direction Velocity V_z/V_{swp} for Various Diversion Rates and Sweeping Velocities at *x* = –0.38, 0, 0.38 m (scales of *y*-axis are different for each figure).

direction, 0.24 m/s in the transverse (*y*-) direction, 0.17 m/s in the vertical (*z*-) direction, and 0.54 m/s for the resultant velocity magnitude. The positive and negative velocity values in Figure 10 show the directionality of the entrainment velocity vectors, which mainly depends on the entrainment starting locations given in Figure 7 of Mussen *et al.* (2013).

The increased knowledge on the hydraulic conditions during the entrainment process, which can be different for different fish species and size classes, is informative in design of fish guidance and protection devices. The entrainment velocity of fish species can be an important design parameter to estimate the inlet area of fish guidance and protection devices. In addition, this knowledge can be coupled with behavioral and physiological data on the species in question to better manage water diversion activities. For example, data on swimming performance has been used to suggest intake velocity limits on water diversions for specific locations within a watershed, and can be integrated with knowledge of ontogeny to provide seasonal limitations as well (*i.e.*, Verhille *et al.*, 2014). Information on specific hydraulic

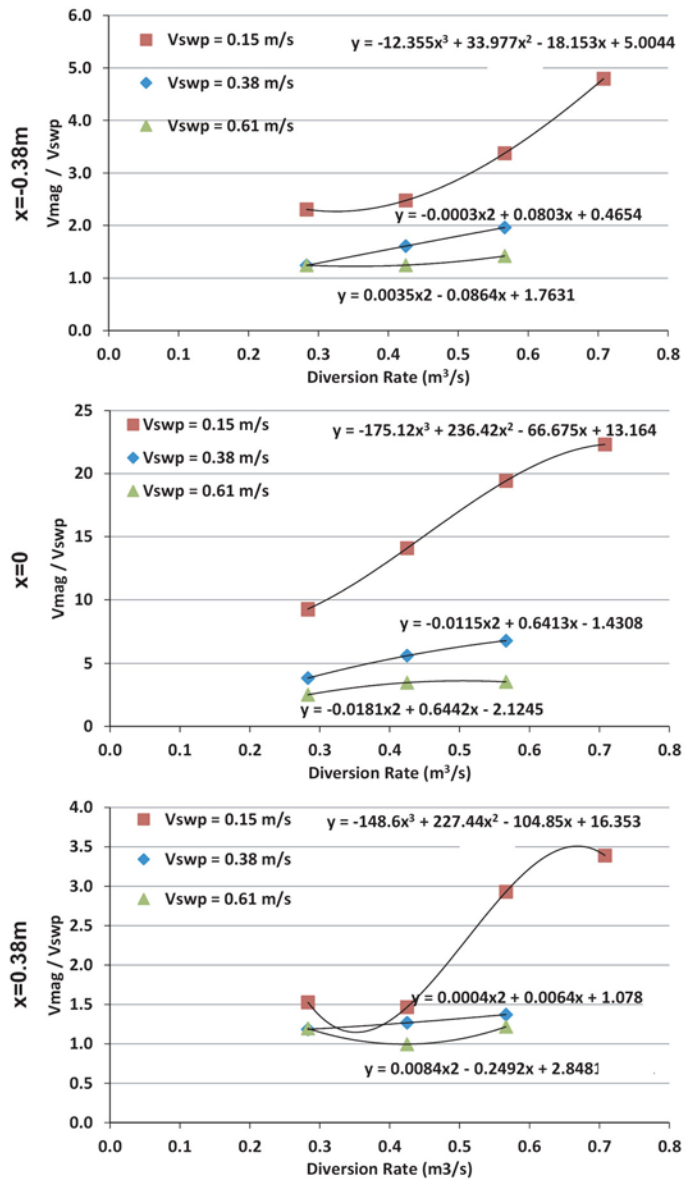

Figure 9. Maximum Values of Nondimensional Velocity Magnitudes V_{mag}/V_{swp} for Various Diversion Rates at x = –0.38, 0, 0.38 m (scales of y-axis are different for each figure).

characteristics surrounding water diversions can therefore help assess ways in which fish can be protected from entrainment by comparing these parameters with the physiological capabilities of fishes, and making adjustments as necessary.

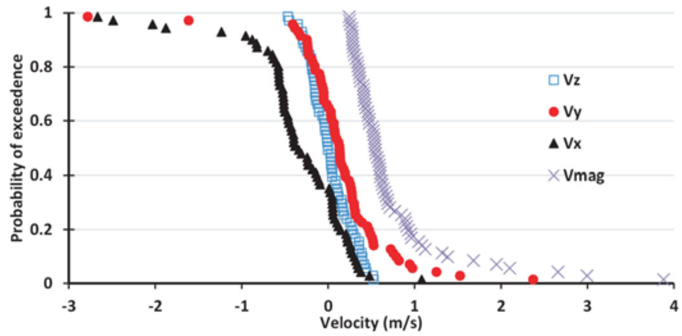

Figure 10. Probability of Exceedance of Juvenile Chinook Salmon Entrainment Velocities in *x*-, *y*-, *z*-Directions and the Corresponding Velocity Magnitudes.

Concluding Remarks

Unscreened diversions, which are commonly used for irrigation purposes, are potentially harmful to migrating and resident fishes. A series of experiments in a large flume were conducted to investigate the hydraulic fields in the vicinity of a 0.46-m-diameter diversion pipe for various diversion rates and channel sweeping velocities. The flow in the diversion pipe was operated by the head difference between the flume and the tail tank, allowing a unique and fish friendly operation without a diversion pump. The experiments showed that all of the velocity components (in longitudinal, transverse, and vertical directions) were significantly greater in the vicinity of the diversion pipe inlet. Therefore, the velocity components in the longitudinal (*x*-), transverse (*y*-), and vertical (*z*-)-directions need to be considered in the modeling and design of fish guidance and protection devices for diversion pipes. Our experimental results should be of great value in understanding the relationships between hydraulic fields and fish swimming behavior near unscreened diversions, and in designing fish-guidance devices to protect fishes from entrainment into unscreened water-diversion pipes. A detailed investigation of the hydraulic fields near diversion pipes with various fish guidance and protection devices is considered a fruitful direction for future research.

Acknowledgments — This research was funded through the U.S. Department of Interior's Anadromous Fish Screen Program (CESU # 3FC810873) and performed at J. Amorocho Hydraulics Laboratory, which was built by the California Department of Water Resources to conduct hydraulic modeling studies for the California State Water Project in the 1960s, at University of California Davis. We thank Matthew Foster, Isela Chavez, Rosbin Barillas, and Roxana Hernandez from the Department of Civil and Environmental Engineering for their assistance with experiments. We also thank Steve Thomas (National Oceanic and Atmospheric Administration's National Marine Fisheries Service) and Dan Meier (U.S. Fish and Wildlife Service) for research recommendations and comments.

Literature Cited

Bowen, M., 2004. Inventory of Barriers to Fish Passage in California's Coastal Watersheds. Coastal Conservancy, Oakland, California. www.calfish.org/Portals/2/Programs/PAD/docs/FPBrochure.pdf *accessed* December 2016.

CalFish (California Cooperative Anadromous Fish and Habitat Data Program), 2012. California Fish Passage Assessment Database. www.calfish.org *accessed* November 2016.

CVPIA (Central Valley Project Improvement Act), 1992. CVPIA: Title 34 of Public Law 102-575. http://www.usbr.gov/mp/cvpia/ *accessed* November 2016.

Gale, S.B., A.V. Zale, and C.G. Clancy, 2008. Effectiveness of Fish Screens to Prevent Entrainment of Westslope Cutthroat Trout into Irrigation Canals. North American Journal of Fisheries Management 28(5):1541-1553, DOI: 10.1577/M07-096.1

Grimaldo, L.F., T. Sommer, N. Van Ark, G. Jones, E. Holland, P.B. Moyle, B. Herbold, and P. Smith, 2009. Factors Affecting Fish Entrainment into Massive Water Diversions in a Tidal Freshwater Estuary: Can Fish Losses Be Managed? North American Journal of Fisheries Management 29(5):1253-1270, DOI: 10.1577/M08-062.1

Herren, J.R. and S.S. Kawasaki, 2001. Inventory of Water Diversions in Four Geographic Areas in California's Central Valley. Fish Bulletin 179:343-355.

Kimmerer, W.J., 2008. Losses of Sacramento River Chinook Salmon and Delta Smelt to Entrainment in Water Diversions in the Sacramento-San Joaquin Delta. San Francisco Estuary and Watershed Science 6(2). http://escholarship.org/uc/item/7v92h6fs *accessed* November 2016.

King, A.J. and J.P. O'Connor, 2007. Native Fish Entrapment in Irrigation Systems: A Step towards Understanding the Significance of the Problem. Ecological Management and Restoration 8 (1):32-37, DOI: 10.1111/j.1442-8903.2007.00329.x

Mussen, T.D., D. Cocherell, Z. Hockett, A. Ercan, H. Bandeh, M.L. Kavvas, J.J. Cech, and N.A. Fangue, 2013. Assessing Juvenile Chinook Salmon Behavior and Entrainment Risk near Unscreened Water Diversions: Large Flume Simulations. Transactions of the American Fisheries Society 142(1):130-142, DOI: 10.1080/00028487.2012.720633

Mussen, T.D., D. Cocherell, O. Patton, D. Jauregui, A. Ercan, H. Bandeh, D. Meier, S. Thomas, M.L. Kavvas, J.J. Cech, and N.A. Fangue, 2015. Modified Water-Diversion Structures Can Behaviorally Deter Juvenile Chinook Salmon from Entrainment. Transactions of the American Fisheries Society 144(5):1070-1080, DOI: 10.1080/00028487.2015.1064476

Mussen, T.D., D. Cocherell, J.B. Poletto, J.S. Reardon, Z. Hockett, A. Ercan, H. Bandeh, M.L. Kavvas, J.J. Cech, and N.A. Fangue, 2014a. Unscreened Water-Diversion Pipes Pose an Entrainment Risk to the Threatened Green Sturgeon, *Acipenser Medirostris*. PLoS ONE 9(1):e86321, DOI: 10.1371/journal.pone.0086321

Mussen, T.D., O. Patton, D. Cocherell, A. Ercan, H. Bandeh, M.L. Kavvas, J.J. Cech, and N.A. Fangue, 2014b. Can Behavioral Fish-Guidance Devices Protect Juvenile Chinook Salmon (*Oncorhynchus tshawytscha*) from Entrainment into Unscreened Water-Diversion Pipes? Canadian Journal of Fisheries and Aquatic Sciences 71(8):1209-1219, DOI: 10.1139/cjfas-2013-0601

Nobriga, M.L., Z. Matica, and Z.P. Hymanson, 2004. Evaluating Entrainment Vulnerability to Agricultural Irrigation Diversions: A Comparison among Openwater Fishes. *In:* Early Life History of Fishes in the San Francisco Estuary and Watershed, Vol. 39, F. Feyrer, L.R. Brown, R.L. Brown, and J.J. Orsi (Editors). American Fisheries Society Symposium, Bethesda, Maryland, pp. 281-295.

Poletto, J.B., D. Cocherell, T.D. Mussen, A. Ercan, H. Bandeh, M.L. Kavvas, J.J. Cech, and N.A. Fangue, 2014. Efficacy of a Sensory Deterrent and Pipe Modifications in Decreasing Entrainment of Juvenile Green Sturgeon (*Acipenser Medirostris*) at Unscreened Water Diversions. Conservation Physiology 2(1):cou056, DOI: 10.1093/conphys/cou056

Poletto, J.B., D. Cocherell, T.D. Mussen, A. Ercan, H. Bandeh, M.L. Kavvas, J.J. Cech, and N.A. Fangue, 2015. Fish Protection Devices at Unscreened Water Diversions Can Reduce Entrainment: Evidence from Behavioral Laboratory Investigations. Conservation Physiology 3(1):cov040, DOI: 10.1093/conphys/cov040

Turnpenny, A.W.H., G. Struthers, and K.P. Hanson, 1998. A UK Guide to Intake Fish-Screening Regulations, Policy and Best Practice. ETSU H/06/0052/00/00. Department of Trade and Industry, Energy Technology Support Unit, Harwell, UK.

Verhille, C.E., J.B. Poletto, D.E. Cocherell, B. DeCourten, S. Baird, J.J. Cech, and N.A. Fangue, 2014. Larval Green and White Sturgeon Swimming Performance in Relation to Water-Diversion Flows. Conservation Physiology, 2(1):cou031, DOI: 10.1093/conphys/cou031

Ali Ercan is Research Associate, **M. Levent Kavvas** is Professor, **Kara Carr** is Assistant Project Scientist, **Zachary Hockett** is Graduate Student, and **Hossein Bandeh** is Staff at Department of Civil and Environmental Engineering, University of California, Davis. **Timothy D. Mussen** is with the Sacramento Regional County Sanitation District, Sacramento, California 95827. **Dennis Cocherell** is Staff Research Associate, **Jamilynn B. Poletto** is a former Postdoctoral Research Fellow, **Joseph J. Cech, Jr.** is Professor Emeritus, and **Nann A. Fangue** is Professor in Department of Wildlife, Fish, and Conservation Biology, University of California, Davis, One Shields Avenue, Davis, California 95616. **Jamilynn B. Poletto** is currently Assistant Professor, School of Natural Resources, University of Nebraska-Lincoln, 3300 Holdrege Street, Lincoln, Nebraska 68583.